Dolgikh, D. A., Gilmanshin, R. I., Brazhnikov, E. V., Bychkova, V. E., Semisotnov, G. V., Venyaminov, S. Yu., & Ptitsyn, O. B. (1981) *FEBS Lett. 136*, 311-315.
Elwell, M., & Schellman, J. A. (1975) *Biochim. Biophys. Acta 386*, 309-323.
Elwell, M., & Schellman, J. A. (1977) *Biochim. Biophys. Acta 494*, 367-383.
Franks, F., & Hatley, R. H. M. (1985) *Cryo-Lett. 6*, 171-180.
Gill, S. J., Nichols, N. F., & Wadso, I. (1976) *J. Chem. Thermodyn. 8*, 445-452.
Greene, R. F., & Pace, C. N. (1974) *J. Biol. Chem. 249*, 5388-5393.
Hatley, R. H. M., & Franks, F. (1986) *Cryo-Lett. 7*, 226-233.
Hawley, S. A. (1971) *Biochemistry 10*, 2436-2442.
Kauzmann, W. (1959) *Adv. Protein Chem. 14*, 1-63.
Kielley, W. W., & Harrington, W. F. (1960) *Biochim. Biophys. Acta 41*, 401-421.
Kuwajima, K., Nitta, K., Yoneyama, M., & Sugai, S. (1976) *J. Mol. Biol. 106*, 359-373.
Lapanje, S. (1973) *FEBS Lett. 31*, 67-69.
Lapanje, S., & Wadso, I. (1971) *Eur. J. Biochem. 22*, 345-349.
Lumry, R., Biltonen, R., & Brandts, J. F. (1966) *Biopolymers 4*, 917-944.
Nojima, H., Ikai, A., Oshima, T., & Noda, H. (1977) *J. Mol. Biol. 116*, 429-442.
Ohgushi, M., & Wada, A. (1983) *FEBS Lett. 164*, 21-24.
Pace, C. N. (1975) *CRC Crit. Rev. Biochem. 3*, 1-43.
Pace, N. C., & Tanford, C. (1968) *Biochemistry 7*, 198-208.
Perry, L. J., & Wetzel, R. (1984) *Science (Washington, D.C.) 226*, 555-557.
Perry, L. J., & Wetzel, R. (1986) *Biochemistry 25*, 733-739.
Perry, L. J., Heyneker, H. L., & Wetzel, R. (1985) *Gene 38*, 259-264.
Pfeil, W., & Privalov, P. L. (1976) *Biophys. Chem. 4*, 33-40.
Privalov, P. L. (1979) *Adv. Protein Chem. 33*, 167-241.
Privalov, P. L. (1982) *Adv. Protein Chem. 35*, 1-104.
Privalov, P. L., Griko, Yu. V., Venyaminov, S. Yu., & Kutyshenko, V. P. (1986) *J. Mol. Biol. 190*, 487-498.
Schellman, J. A. (1958) *C. R. Trav. Lab. Carlsberg 30*, 395-414.
Schellman, J. A. (1978) *Biopolymers 17*, 1305-1322.
Schellman, J. A. (1987) *Annu. Rev. Biophys. Biophys. Chem. 16*, 115-137.
Schellman, J. A., & Hawkes, R. B. (1980) in *Protein Folding* (Jaenicke, R., Ed.) pp 331-341, Elsevier/North-Holland, New York.
Schellman, J. A., Lindorfer, M., Hawkes, R., & Grutter, M. (1981) *Biopolymers 20*, 1989-1999.
Sturtevant, J. M. (1987) *Annu. Rev. Phys. Chem. 38*, 463-488.
Tanford, C. (1968) *Adv. Protein Chem. 23*, 121-282.
Wetzel, R., Perry, L. J., Baase, W. A., & Becktel, W. J. (1988) *Proc. Natl. Acad. Sci. U.S.A. 85*, 401-405.
Wong, K. P., & Tanford, C. (1973) *J. Biol. Chem. 248*, 8518-8523.
Zipp, A., & Kauzmann, W. (1973) *Biochemistry 12*, 4217-4228.

Low-Temperature Unfolding of a Mutant of Phage T4 Lysozyme. 2. Kinetic Investigations†

Bao-lu Chen,‡ Walter A. Baase, and John A. Schellman*
Institute of Molecular Biology and Department of Chemistry, University of Oregon, Eugene, Oregon 97403-1229
Received June 14, 1988; Revised Manuscript Received August 18, 1988

ABSTRACT: A disulfide-bridged variant of bacteriophage T4 lysozyme has been found to undergo a low- as well as high-temperature unfolding transition in guanidinium chloride [see Chen and Schellman (1989)]. The kinetics for this process have been followed for several temperatures, a range of guanidinium chloride concentrations, and a number of values of pH. Microscopic rate constants for protein unfolding and refolding were extracted from these data to explore the nature of the cold unfolding transition. The data were interpreted using transition-state theory. It was found that the Arrhenius energy is temperature dependent. The transition state is characterized by (1) a high energy and low entropy compared to the native state, (2) a heat capacity which is closer to the native state than to the unfolded state, and (3) a low exposure to solvent compared to the unfolded state, as judged by its interaction with guanidinium chloride. With increasing concentration of guanidinium chloride, the low-temperature unfolding rate increases strongly, and the refolding rate decreases very strongly.

The background of this research was described in the previous paper (Chen & Schellman, 1989), hereafter referred to as paper 1, which discusses the equilibrium study of the reversible, low-temperature unfolding of the disulfide-bridged T4 lysozyme mutant I3C-C97/C54T. Moderately concentrated guanidinium chloride is required to bring the low-temperature transition into a temperature region where it can be observed. The rates of unfolding and refolding are very slow as temperatures of 0 °C and below are approached, and this suggested the possibility of an extensive kinetic investigation. The reaction rates are sufficiently slow so that the kinetic studies can be performed with a conventional circular dichrometer with no need for fast techniques.

Such a study has a number of attractive possibilities. With slow reaction rates, it is conceivable that one could see pro-

†This work has been supported by NIH Grant GM20195 and by NSF Grant 8609113.
‡Present address: Department of Biology, Massachusetts Institute of Technology, 77 Massachusetts Ave., Cambridge, MA 02139.

0006-2960/89/0428-0691$01.50/0

cesses that elude investigation when fast kinetic methods must be used. In addition, the low-temperature unfolding reaction has been observed rather rarely, its equilibrium thermodynamics are unusual, to say the least, and a comparison of these reactions with their high-temperature counterparts could throw a different light on the problems of protein folding and stability. Finally, most of our work on mutants of T4 lysozyme has been restricted to equilibrium measurements. This was a good opportunity to enlarge our approach to this problem by including the study of rates.

This type of study is far from new. Tanford and his coworkers observed the slow unfolding and refolding of β-lactoglobulin at low temperatures in urea and guanidine solutions (Pace & Tanford, 1968; Takagi & Tanford, 1968). They found the rate was first order in urea but multistep in guanidinium solutions (Tanford, 1968) and did not pursue the kinetic investigation further. Some of the T4 lysozyme mutants unfold and refold much more cleanly and reversibly than β-lactoglobulin at low temperature under similar conditions (Chen, 1988). The I3C-C97/C54T system appeared to be ideal for a study that would include a search for intermediates and an investigation of the effects of point mutations, denaturing agents, and temperature on the unfolding and refolding rates of a protein. The present study is a prototype investigation of the single protein I3C-C97/C54T.

Experimental Procedures

The source of purified T4 lysozyme (I3C-C97/C54T), materials, and instrumentation are described in the preceding paper (Chen & Schellman, 1989).

Sample pH was maintained primarily by 2 mM phosphate buffer. Occasionally, 10 mM sodium acetate was used as the buffer for experiments done near pH 4.5 and 10 mM Tris·HCl for pH above 7. There was no detectable difference in the equilibrium or kinetic measurements among these buffers.

Concentration-jump and temperature-jump methods were used to follow the kinetics of this system. The temperature-jump methods, which brought the system from one thermal equilibrium to another, were done directly with the HP89100A thermal controller. In the temperature range of this study, the controller shifted the sample temperature with a half-time of 30–60 s. The concentration-jump method was applied to study transitions from the fully native and fully unfolded states. The procedure for the unfolding experiment from the native state was to add 44 μL of protein stock (1.30 mg/mL) to 2.45 mL of precooled, buffered solvent and to follow the kinetics by recording the CD signal. For the refolding experiment from the fully unfolded state, 44 μL of protein stock was first added to 1.0 mL of buffered 7.5 M Gdn·HCl and allowed to denature overnight at 4 °C. It was then chilled to the experimental temperature and mixed with cooled water to adjust the Gdn·HCl concentration to 3 M, and the kinetics were immediately recorded. The time base for all measurements was provided by the HP87XM computer.

Kinetic data were fitted to a first-order exponential using a weighted least-squares subroutine from Bevington (1969). Data were collected for at least seven relaxation times, i.e., 7τ, to ensure that the equilibrium plateau was reached. The data were analyzed to 90% completion of the reaction, i.e., 2.3τ.

Results

Our initial aim was to survey the dependence on temperature of the forward and backward rates of the folding reaction

$$N \underset{k_2}{\overset{k_1}{\rightleftharpoons}} D \qquad (1)$$

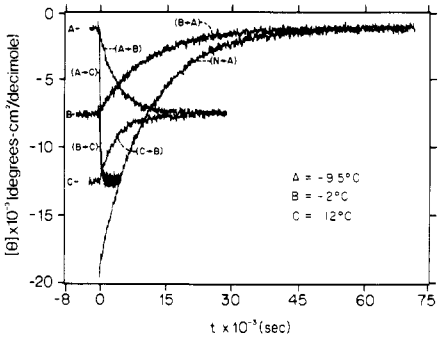

FIGURE 1: Kinetics of the unfolding and refolding of I3C-C97/C54T T4 lysozyme in 3 M Gdn·HCl at pH 6.32, monitored by circular dichroism at 223 nm. Five curves are the results of temperature-jump experiments: B → A, −2 to −9.5 °C; C → B, 12 to −2 °C; A → B, −9.5 to −2 °C; A → C, −9.5 to 12 °C; B → C, −2 to 12 °C. The sixth curve, N → A, is the result of a concentration-jump experiment, mixing native protein with 3 M Gdn·HCl at −9.5 °C.

at fixed guanidinium chloride concentration (3 M). N is the folded or native form, and D is the unfolded or denatured form. The purpose was to establish an overall profile of the kinetic picture and to check for the presence of kinetic intermediates. Three temperatures were chosen: −9.5 °C, close to the lowest accessible temperature at this guanidinium concentration (3 M); −2 °C, a temperature close to the middle of the low-temperature transition; and 12 °C, a temperature near the point of maximum stability (see Figure 2 of paper 1). The results of rate experiments at these temperatures are shown in Figure 1. The horizontal bars on the left of the figure represent the equilibrium values of the circular dichroism (223 nm) at the three temperatures, −9.5, −2.0, and 12 °C, labeled A, B, and C, respectively. Five of the curves are essentially T-jump experiments where the protein at equilibrium at one temperature was brought to another temperature during a time interval short compared with the relaxation time of the system. These curves are labeled A → B, A → C, etc. It is to be understood that the curves were collected at the final temperatures, −2 and 12 °C, in these examples. The last curve, labeled N → A, was obtained by mixing a native protein stock solution with a guanidinium chloride solution to form a 3 M solution of denaturant at −9.5 °C. Experiments like these permitted the determination of the forward and reverse kinetic rates at the selected temperatures. It is to be noted that the final value of the circular dichroism in the experiments was independent of the direction of the reaction within experimental error. This is evidence for the reversibility of the reaction.

The kinetics under these conditions are independent of the protein concentration in the range used in this work (0.01–0.03 mg/mL). The relaxation time, τ, for these systems was evaluated by plotting the extent of reaction, $\ln \{[CD(t) - CD(\infty)]/[CD(0) - CD(\infty)]\}$, versus the time, t (Ikai & Tanford, 1973), where $CD(t)$ represents the circular dichroism at 223 nm at time t while 0 and ∞ denote respectively the initial time and a very long time at which the reaction approaches completion. The results of this analysis are shown in Figure 2. The plots are linear, as were all similar plots for this protein under the conditions of temperature and guanidinium concentrations used in this study. The linear plots of Figure 2 permit the evaluation of a relaxation time, τ, for each curve using the representation $CD(t) - CD(\infty) = CD(0) - CD(\infty) \exp(-t/\tau)$. As can be seen from Figure 2, the relaxation times are the same, within experimental error, for the forward and backward reactions, irrespective of initial conditions. Thus, for the experimental conditions cited, the re-

Table I: Temperature Dependence of Transition-State Thermodynamic Parameters Using Data of Figure 3 and Equations 2 and 4[a]

T (°C)	$\Delta\bar{G}^{\ddagger}_1{}'$[b]	$\Delta\bar{H}^{\ddagger}_1{}'$	$\Delta\bar{S}^{\ddagger}_1{}'$	$\Delta\bar{G}^{\ddagger}_2{}'$[c]	$\Delta\bar{H}^{\ddagger}_2{}'$	$\Delta\bar{S}^{\ddagger}_2{}'$
-9.5	20.2	7.12	-49.7	21.3	57.1	136
-2	20.5	11.2	-34.3	20.4	44.9	90.1
12	20.8	18.9	-6.78	19.7	22.0	7.90

[a] Units: $\Delta\bar{G}^{\ddagger}{}'$ and $\Delta\bar{H}^{\ddagger}{}'$ in kilocalories per mole; $\Delta\bar{S}^{\ddagger}{}'$ in calories per mole per degree Kelvin. [b] $\Delta C_{p_1}{}^{\ddagger}{}' = 547$ cal/(mol·K). [c] $\Delta C_{p_2}{}^{\ddagger}{}' = 1634$ cal/(mol·K).

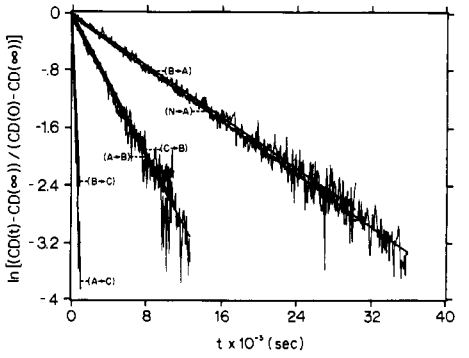

FIGURE 2: Logarithmic transformation and two-state linear fits of the kinetic data in Figure 1. In the logarithmic transformation of the ordinate, CD(0) is the average of the equilibrium data before zero time at which the temperature-jump experiment begins or the first data point for the mixing experiment, CD(∞) is the average over the final plateau of the kinetic run, and CD(t) is the data from zero time to 90% completion of the reaction.

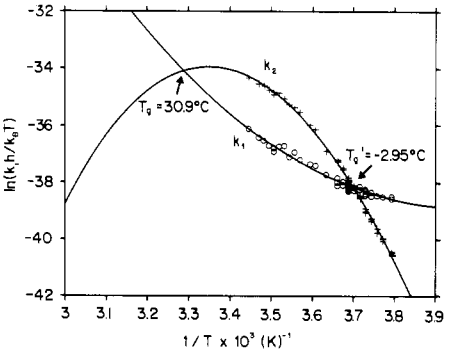

FIGURE 3: Temperature dependence of the intrinsic unfolding and refolding rate constants in 3 M Gdn·HCl at pH 5. The ordinate is the logarithmic transformation of the microscopic rate constants into activation equilibrium constants. The abscissa is the reciprocal of the absolute temperature. (○) is for the unfolding rate constant k_1, and (+) is for the refolding rate constant k_2. The continuous lines are the fitting results according to eq 4 with $T_0 = 270.15$ K.

action is evidently two-state with at most only a low population of the intermediate states.

Equilibrium constants were also evaluated for these experiments (see paper 1) so that rate constants for the unfolding reaction, k_1, and for the refolding reaction, k_2, could be evaluated by using the standard relations $K' = k_1/k_2$ and $1/\tau = k_1 + k_2$. The prime on the equilibrium constant is a reminder of the presence of guanidinium chloride in these experiments (see paper 1). Plots of ln (hk_1/k_BT) and ln (hk_2/k_BT) vs $1/T$ are shown in Figure 3, where h and k_B are Planck's and Boltzmann's constants, respectively. The two crossover points, where $k_1 = k_2$, are the high and low melting temperatures of the protein. The solid curves are the result of a least-squares analysis described below. The plots are not linear, though that for k_1 is almost so, indicating that the data cannot be described in terms of a simple, constant Arrhenius energy. Pohl (1968) has discussed the unfolding and refolding kinetics of several proteins which have single relaxation time kinetics for their normal high-temperature unfolding reactions. These proteins show curvature in their Arrhenius plots for ln k_2, but the ln k_1 plots tend to be linear. Segawa and Sugihara (1984) have reported a detailed study of the kinetics of the high-temperature unfolding of hen egg white lysozyme in the presence of denaturing agents. They also found curved Arrhenius plots for ln k_2 but linear plots for ln k_1. We will compare our results with those of these workers under Discussion. Desmadril and Yon (1984) have reported kinetic intermediates in the high-temperature unfolding of the wild-type T4 lysozyme. This is in contrast with the low-temperature melting of I3C-C97/C54T described here which shows single-step kinetics. These T4 lysozymes are, however, significantly different from one another because of the presence of a large loop bridged by the -S-S- bond in I3C-C97/C54T as well as the absence of free thiol groups.

The kinetic data were analyzed by using transition-state theory via the Eyring equation [e.g., see Laidler (1950)]:

$$\Delta\bar{G}^{\ddagger}_i = -RT \ln K^{\ddagger}_i = -RT \ln (k_i h/k_B T) \qquad (2)$$

where i is 1 or 2 for the reactions of eq 1. Our analysis consists of a literal interpretation of $\Delta\bar{G}^{\ddagger}_i$ as a thermodynamic quantity, which is to be analyzed in the same manner as $\Delta\bar{G}$ for the equilibrium reaction. Since $\Delta\bar{C}_p$ is large for the two-state transition N $\rightleftharpoons$ D, and since any partial molar property, $\bar{J}$, of the protein must follow the rule

$$\Delta\bar{J} = \bar{J}_D - \bar{J}_N = (\bar{J}^{\ddagger} - \bar{J}_N) - (\bar{J}^{\ddagger} - \bar{J}_D) = \Delta\bar{J}^{\ddagger}_1 - \Delta\bar{J}^{\ddagger}_2 \qquad (3)$$

where $\bar{J}^{\ddagger}$ refers to an intermediate state, it would be inconsistent with the transition-state concept to ignore $\Delta\bar{C}_{p_1}{}^{\ddagger}$ and $\Delta\bar{C}_{p_2}{}^{\ddagger}$. Looked at from this viewpoint, the curvature of the Arrhenius plots in Figure 3 is to be expected. As with the equilibrium case, we assume the constant $\Delta\bar{C}_{p_i}{}^{\ddagger}$ model (see eq 12 of paper 1). By direct analogy:

$$\ln K^{\ddagger}_i{}' = A_i + B_i(T_0/T) + C_i \ln (T_0/T) \qquad (4)$$

with the coefficients

$$A_i = [-\Delta\bar{C}_{p_i}{}^{\ddagger} + \Delta\bar{S}^{\ddagger}_i(T_0)]/R$$

$$B_i = [\Delta\bar{C}_{p_i}{}^{\ddagger} - \Delta\bar{S}^{\ddagger}_i(T_0)]/R - \Delta\bar{G}^{\ddagger}_i(T_0)/RT_0$$

$$C_i = -\Delta\bar{C}_{p_i}{}^{\ddagger}/R$$

where $i = 1$ or 2 for the forward or backward reaction, respectively. We have dropped the primes on these thermodynamic quantities because of the complexity of the notation. A_i, B_i, and C_i were evaluated by means of a program for nonlinear regression [see paper 1 and Chen (1988)]. Analysis of the results is shown in Table I, and the interpretation of these data will be deferred to the Discussion.

All of the above results were obtained in 3.00 M guanidinium chloride, and the next task was to determine the effect of C_3, the denaturant concentration, on the rates. The natural logs of the relaxation times as a function of guanidinium concentration are shown in Figure 4. Such plots in general give a "∧"-shaped curve (Ikai et al., 1973; Crisanti & Matthews, 1981; Matthews & Hurle, 1987) with a maximum near C_m, where $k_1 = k_2$. The left branch of the curve is dominated by $1/k_2$ and the right by $1/k_1$. Because of freezing of solutions at low temperatures, and rates too fast to measure at high temperatures, our measurements were confined to the relatively

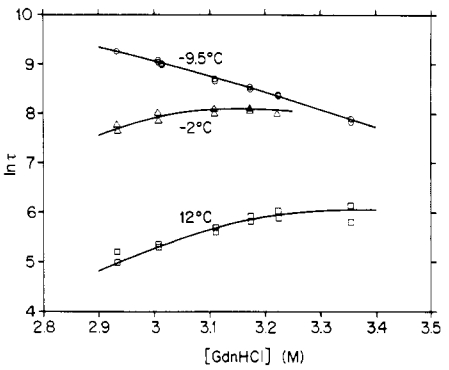

FIGURE 4: Natural log of relaxation times as functions of Gdn·HCl molarity at pH 5 and three temperatures: −9.5 °C, (○), −2 °C (△), and 12 °C (□). The continuous lines are the simulation lines based on the relation $\tau = 1/(k_1 + k_2)$ with the assumption of $\ln k_i = a_i + b_i C_3$.

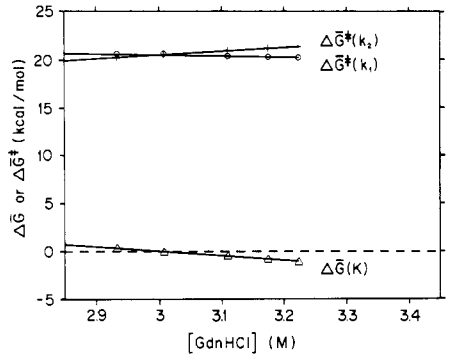

FIGURE 5: Activation free energy change of unfolding (○) and refolding (+) and free energy change of unfolding (△) as functions of the molar concentration of Gdn·HCl at −2 °C and pH 5.

Table II: Solvent Dependence of Transition-State Thermodynamics of I3C-C97/C54T in Gdn·HCl at pH 5 Using Equation 5[a]

		12 °C	−2 °C	−9.5 °C
k_1	$\Delta\bar{G}^{\ddagger}_1$	23500	23600	25800
	$RT(\beta^{\ddagger} - \beta_N)$	−980	−1040	−1890
k_2	$\Delta\bar{G}^{\ddagger}_2$	10300	9250	16000
	$RT(\beta^{\ddagger} - \beta_D)$	3170	3740	1780

[a] Units: $\Delta\bar{G}^{\ddagger}_i$ in calories per mole; $RT(\beta^{\ddagger} - \beta_i)$ in calories per mole squared.

small segments of the entire curve shown in Figure 4.

For each guanidinium concentration, k_1 and k_2 were calculated from the equilibrium constant and τ, converted to $\Delta\bar{G}^{\ddagger}_i'$, and plotted as a function of guanidinium concentration, C_3. The results for −2 °C are shown in Figure 5. The plots were all linear within the error of the experiments and could be represented by the equation:

$$\Delta\bar{G}^{\ddagger}_i' = \Delta\bar{G}^{\ddagger}_i + RT(\beta^{\ddagger} - \beta_i)C_3 \qquad (5)$$

Slopes, $RT(\beta^{\ddagger} - \beta_i)$, and intercepts, $\Delta\bar{G}^{\ddagger}_i$, of the least-squares straight lines are given in Table II. Because of the long extrapolation, we have limited confidence in the physical interpretation of the $\Delta\bar{G}^{\ddagger}_i$ values as activation free energies in the absence of guanidine, except as a rough indication. On the other hand, the slopes of the lines are a measure of the nature and intensity of the interaction between the protein and the denaturing agent (Schellman, 1978). A negative sign indicates that the transition state interacts more strongly with the denaturant than the initial state (N or D) and vice versa. The magnitude of $RT(\beta^{\ddagger} - \beta_i)$ is an indicator for the magnitude of the relative interaction. In Table I, the data at −9.5 °C are less reliable than the other data because the protein

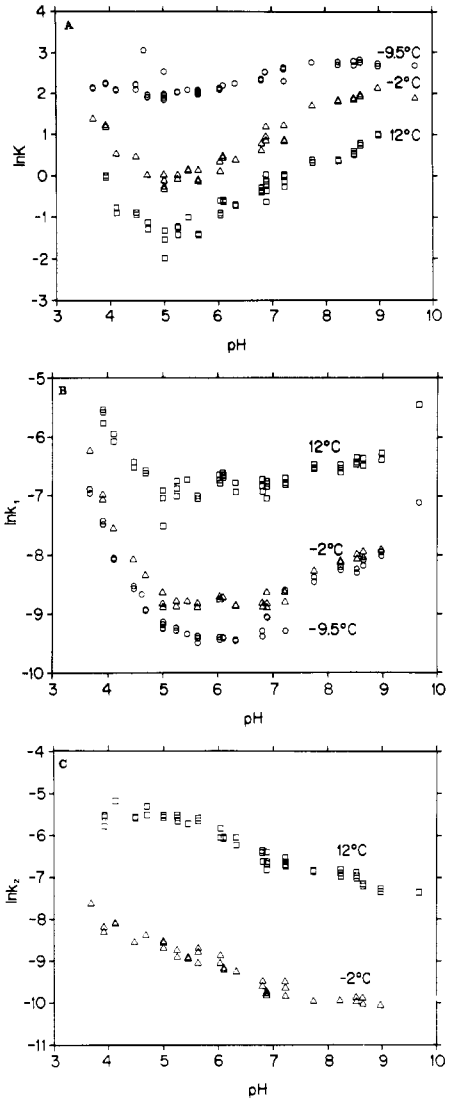

FIGURE 6: Dependencies in 3 M Gdn·HCl of the equilibrium constant for unfolding, K' (A), and the intrinsic rate constant of unfolding, k_1 (B), and of refolding, k_2 (C), on pH at temperatures −9.5 (○), −2 (△), and 12 °C (□).

is always mostly unfolded at this temperature. All of the data are too close to the base line of the unfolded protein, and this leads to inaccurate experiments.

Rates and equilibria were determined as a function of pH in 3 M guanidinium chloride at the three selected temperatures. The results are shown in Figure 6A–C. The curve for k_2 at −9.5 °C has been eliminated from Figure 6C for the following reasons. The equations for $\ln k_1$ and $\ln k_2$ can be written in the form:

$$\ln k_1 = \ln (1/\tau) - \ln (1 + 1/K') \qquad (6a)$$

$$\ln k_2 = \ln (1/\tau) - \ln (1 + K') \qquad (6b)$$

$1/\tau$ is essentially k_1 when K is very large, and essentially k_2 when K is very small. Conversely, it is very difficult to determine k_1 at small K or k_2 at large K. The following criteria appear to be in accordance with the accuracy of our experiments and have been adopted to avoid overinterpretation of the data: for $\ln K' > 2$, k_2 is inadequately determined and for $\ln K' < -2$, k_1 is inadequately determined. At −9.5 °C, we consider k_2 to be undetermined and K' only approximately determined. There is a maximum in the stability of the protein (minimum in K') near pH 5–6. This is to be compared with the stability maximum at pH 5.5 found by W. A. Baase and

W. J. Becktel (personal communication) for this same protein by studying its high-temperature melting in the absence of guanidinium salts.

It is to be noted that k_2 decreases monotonically as the pH increases, while k_1 goes through a minimum at about pH 5. These results will be discussed below.

Discussion

Proline Isomerization. The domination of the data by a single relaxation time for the forward and backward reactions indicates that there is no slow refolding step associated with proline isomerization (Garel & Baldwin, 1973; Brandts et al., 1975). T4 lysozyme has three proline residues at positions 37, 86, and 143, and all are trans (Weaver & Matthews, 1987). Even with only a 10% probability per residue for the cis form in the unfolded state, the probability of a cis mismatch would be 27%. It is possible that the cis–trans isomerism is too slow or too fast compared to our long relaxation times, but an extrapolation of the data of Grathwohl and Wuthrich (1981) down to 0 °C gives a relaxation time of 7.5 min, which is the same order as the reaction rate. Segawa and Sugihara (1984) have performed an analysis of the problem [see also Utiyama and Baldwin (1986)]. They found that a slow-folding component with an amplitude of 10% of the fast-folding amplitude would not be detectable within the experimental error of their measurements. It would be difficult to rule out this possibility on the basis of the data of Figure 2. We did look at a large number of plots like those in Figure 2 to see whether the curve for refolding fell consistently above the curve for unfolding. This would occur if there were a slow reaction with too small an amplitude to detect as a separate exponential, but large enough to be seen above the experimental error. No such trend was observed. Both equilibrium and kinetic aspects of proline cis–trans isomerism are known to depend on neighbors in the polypeptide chain (Grathwohl & Wuthrich, 1981). Segawa and Sugihara have found that the isomerization does not play a noticeable role in the refolding kinetics of hen egg white lysozyme. Evidently, the low-temperature unfolding of this mutant of T4 lysozyme is another such case. In a later publication [see also Chen et al. (1988)], we will report a study of the effect of adding and deleting prolines from T4 lysozyme by site-directed mutagenesis, which addresses this question.

Thermodynamic Reaction Profiles. The fact that I3C-C97/C54T unfolds and refolds cleanly and reversibly with a single relaxation time for each experimental condition has permitted us to accumulate a large amount of data on the effect of temperature, denaturant concentration, and pH on the rates of the forward and backward reaction. The data do not follow the Arrhenius law for temperature variation and should not be expected to do so. If the transition state is considered to be an intermediate state characterizable by thermodynamic properties, then there must be changes in the heat capacity from the native state to the transition state ($\Delta\bar{C}_{p_1}{}^{\ddagger}$) and from the transition state to the unfolded state ($-\Delta\bar{C}_{p_2}{}^{\ddagger}$), because the total change in $\Delta\bar{C}_p$ must be the same in going through the transition state as it is in going directly from the N state to the D state (see eq 3). This leads to curvature in the Arrhenius plots.

In this section, we will see what conclusions can be drawn from a literal application of transition-state theory, which we construe along the lines outlined by Northrup et al. (1982). Protein unfolding is a much more complex transformation than the localized protein processes considered by Northrup et al., and the reaction barrier undoubtedly has a very high dimensionality because of the extensive, and perhaps global, motions of atoms in the formation of the activated complex. There may even be more than one pathway, though the free energies of the transition states of different pathways would have to be very close to one another because of the exponential dependence on $\Delta\bar{G}^{\ddagger}$. The transmission coefficient, κ, has been taken as unity in eq 2 since there is no knowledge of its probable value for a reaction of this type. Errors in the estimation of the thermodynamics of the transition state depend on $\ln \kappa$ and may not be large. There is no known way to certify the physical reality of the parameters determined by the transition-state theory, and we will simply assume that the numbers that we get from the analysis are a reflection of the changes in thermodynamic properties as the protein goes from one of its stable states to the rate-determining intermediate state. In the long run, the use of the Eyring formula with the elementary barrier-crossing coefficient, $k_B T/h$, will have to be justified by the correctness and consistency of the conclusions that are drawn from the analysis.

We assume that the variation of $\Delta\bar{H}^{\ddagger}_i$ with temperature is linear; i.e., $\Delta\bar{C}_{p_i}{}^{\ddagger}$ is constant, so that the thermodynamic model for the transition state is identical with that which we have used for the equilibrium reaction in paper 1. The parameters A_i, B_i, and C_i of eq 4, obtained by fitting the data of Figure 3, lead to the results shown in Table I. These results permit the calculation of the reaction profiles of a number of the thermodynamic parameters for the system (Figure 7A–C). These calculated properties are susceptible to greater errors than the original kinetic data, and we do not claim that they have been accurately determined. We do assume that they are qualitatively correct, however. For example, the small curvature associated with the plot for k_1 in Figure 3, which is opposite in sign to the larger curvature associated with the plot for k_2, leads directly to the picture of $\Delta\bar{C}_p{}^{\ddagger}$ given in Figure 7.

We do not present a profile plot of $\Delta\bar{G}$. Its behavior is best seen in Table I which shows that $\Delta\bar{G}^{\ddagger}_1$ increases slowly with temperature while $\Delta\bar{G}^{\ddagger}_2$ decreases, and from Figure 5 which shows that $\Delta\bar{G}^{\ddagger}_1$ decreases with increasing guanidinium counterion whereas $\Delta\bar{G}^{\ddagger}_2$ strongly increases.

Figure 7A shows the profile for $\Delta\bar{C}_p$. It is monotonic, increasing as one goes from N to the transition state to D. The increase in $\Delta\bar{C}_p$ which accompanies the unfolding of proteins is generally considered to arise from the interaction of exposed hydrophobic groups with water (Privalov, 1979), though there may be large contributions from the increase in vibrational entropy (Sturtevant, 1977; Hawkes et al., 1984) and from the hydration of polar groups (Careri et al., 1980). For a recent discussion, see Baldwin (1986). Whatever is measured by $\Delta\bar{C}_p$, our results show that the transition state is about 25% on the way to the unfolded state with respect to this parameter. If we subscribe to the conventional dictum relating $\Delta\bar{C}_p$ to the disruption of hydrophobic interactions, then the transition state is about 25% on the way to this change in solvation. It would not be correct, however, to state that 25% of the hydrophobic surface area or 25% of the number of hydrophobic side chains have been exposed. Protein side chains are quite heterogeneous and do not contribute to the totality of the hydrophobic effect in a proportionate manner.

Plots of $\ln k_1$ and $\ln k_2$ vs $1/T$ have been compared by Pohl (1968) and by Segawa and Sugihara (1984) for high-temperature unfolding. The proteins considered were trypsinogen, trypsin, chymotrypsinogen A, α-chymotrypsin, elastase, and ribonuclease by Pohl and hen egg white lysozyme by Segawa and Sugihara. These authors found the $\ln k_1$ plots to be linear but the $\ln k_2$ plots to be curved. This conclusion is in qualitative agreement with our finding of small and large curva-

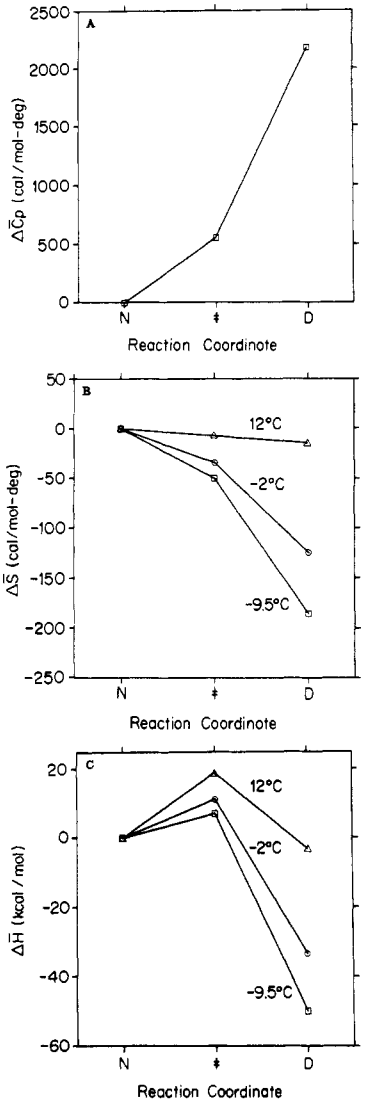

FIGURE 7: Reaction profile of the unfolding process for I3C-C97/C54T T4 lysozyme in 3 M Gdn·HCl at pH 5. The abscissa indicates that the reaction proceeds from native state "N" to transition state "‡" and then to denatured state "D". The ordinates indicate the change in heat capacity (A), entropy (B), and enthalpy (C). The reference points are arbitrarily set at the native state. Data are presented for entropy and enthalpy at temperatures of −9.5 (□), −2 (○), and 12 °C (△).

tures, respectively. This means that $\Delta\bar{C}_p^{\ddagger}$ is small or zero for the passage from the folded state to the transition state for the cited proteins. In light of the discussion above, this could indicate that there is little net breakage of hydrophobic interactions in the transition state. A transition state which is compact and maintains most of the hydrophobic interactions of the native state is in accordance with a number of theoretical models for protein unfolding (Goldenberg & Creighton, 1985).

Approximate reaction profiles for $\Delta\bar{S}$ and $\Delta\bar{H}$ are shown in panels B and C of Figure 7, respectively. These are shown at the three selected temperatures with the native form set to zero as the reference state in each case. We see in Figure 7B that the entropy is monotonic, becoming increasingly negative in the passage through the transition state to the unfolded state. There are not many known sources of negative entropy for an unfolding reaction aside from the hydrophobic effect, so we attribute the sign of the entropy change to the domination by the entropy of disrupting hydrophobic interactions. Figure 7B shows further that the magnitude of the entropy changes becomes smaller as the temperature is raised from −9.5 to 12

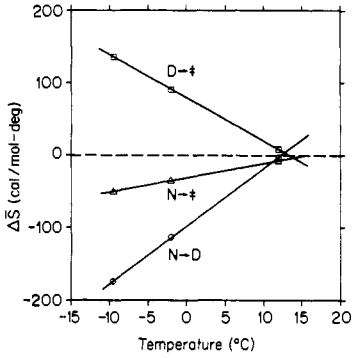

FIGURE 8: Dependence of the entropy of activation and unfolding on temperature. The curves are unfolding (○), unfolding activation process (△), and refolding activation process (□).

°C. This is illustrated more clearly in Figure 8 which shows the three entropy changes plotted as a function of temperature. The entropy changes extrapolate to zero at about 12 °C. The temperature of maximum stability, T_s, of the protein under the given solvent conditions where $\Delta\bar{S}$ equals zero is about 12.5 °C (paper 1). The graphs show that the activation entropies also extrapolate to zero at approximately the same temperature. Note that only two of the curves are independent.

An explanation for the zero equilibrium entropy change at T_s was proposed by Brandts (1964) and may be paraphrased as follows. The entropy of unfolding has a large negative hydrophobic component and a number of other components which should be positive, for example, the disordering of the secondary and tertiary structures. As the temperature is raised, the hydrophobic contribution decreases in magnitude, extrapolating to zero above 100 °C (Baldwin, 1986). At low temperature, the hydrophobic contributions dominate, while at high temperature the positive components dominate. In between, a temperature (T_s) is reached where there is exact balance.

Figure 8 shows that the entropy of the activation processes goes to zero at essentially the same temperature as the equilibrium process for this protein and experimental conditions. This result was not expected. A possible but far from compelling explanation is that the passage from the folded to the transition state is a miniature version of the total unfolding as far as entropy changes are concerned. What this means structurally is uncertain since there is no direct correlation between entropy changes and structure. We cannot deduce from these entropy changes any information about the extent to which the secondary structure has unfolded in the transition state, nor to what extent the activated molecule is compact or extended except in terms of a model. If this type of behavior proves to be general, it should provide an interesting clue to the nature of the transition state for unfolding, but for the present, we are dealing with just one set of results.

The enthalpy profile (Figure 7C) reveals the unusual feature that the enthalpy of activation for unfolding is opposite in sign to the entropy of activation. Practically all processes which are related to the stability of proteins, e.g., thermal transitions, effects of mutations, hydrophobic interactions, etc., are compensatory in nature; i.e., the enthalpy and the entropy are of the same sign so that the two components of the free energy, ΔH and $T\Delta S$, tend to cancel. The formation of the transition state from the folded state at low temperature is the only exception that has been observed in our experience. According to conventional interpretation $\Delta C_{p_1}^{\ddagger}$ and $\Delta S^{\ddagger}_1$ are dominated by the hydrophobic effect and display positive and negative values, respectively. If $\Delta H^{\ddagger}_1$ were also dominated by the hydrophobic effect, it would also be negative like ΔH of un-

folding. The results indicate that there is a real energetically disruptive process in the formation of the transition state from the folded state, presumably to raise the energy of the protein above the low value that is predicted by all energy minimization and molecular dynamics calculations. This could be a breakdown in tertiary structure, i.e., the breakup of a fraction of the nonbonded and energetically favorable side chain interactions which are responsible for the stabilization of the protein; it could be a partial melting of a fraction of the protein, both tertiary and secondary structure etc. As a result, the high barrier to unfolding is a synergistic effect of the positive enthalpy and negative entropy of formation of the transition state from the folded form.

The high barrier for refolding, on the other hand, is caused by the very large positive enthalpy which is in fact counteracted by positive entropy which aids refolding. The activation process for the refolding reaction has simultaneously a large negative ΔC_p, a large positive ΔH, and a large positive ΔS. These changes are textbook indicators for the formation of hydrophobic interactions, and we assume that the passage from the D to the transition-state form and its reverse is dominated by the making and breaking of hydrophobic interactions, respectively.

Dependence on Guanidinium Concentration. The rapid rise of k_1 with increasing concentration of guanidinium ion indicates the stabilization of the transition state relative to the native state. In a thermodynamic interpretation of the transition state, the change in free energy of activation caused by the presence of a denaturing agent is attributed to the relative change of the excess free energy functions of the two states. The formalism of Schellman (1978) may be applied to the transition state relative to the N or D states, since it depends only on a comparison of two well-defined states (Matthews & Hurle, 1987). Accordingly, apparently linear plots like those shown in Figure 5 are examples of the "linear model" applied to transition states, and the slope, $RT(\beta^{\ddagger} - \beta_N)$, is a measure of the relative interaction of N and the transition state with the denaturant. The fact that the coefficient of C_3 is negative indicates the interaction is stronger with the transition state than the native state. This provides a reasonable picture of a transition state which has been partially opened so that there is an increased exposure of groups to the surrounding medium. $RT(\beta^{\ddagger} - \beta_N)$ is about 20% of the value for the complete unfolding of the molecule, $RT(\beta_D - \beta_N)$. This gives a rough idea of the extent of exposure of groups in the transition state, but this information should be used with care. If the exposed groups interact more strongly than the average for the entire protein, then less than 20% exposure is indicated, and the opposite is true if the exposed groups interact more weakly than the average.

The picture is quite different for the refolding reaction in Figure 5. Here the slope, $RT(\beta^{\ddagger} - \beta_D)$, is positive, indicating a stronger interaction of the unfolded protein with guanidine than the transition state. This corresponds with a physical picture in which contacts between solvent and protein groups must be eliminated to make way for the protein–protein contacts which exist in the transition state. The lower the concentration of guanidinium chloride, the easier it is to eliminate solvent from the protein groups and the lower the free energy barrier for the refolding reaction. The refolding reaction is evidently very fast in the absence of guanidinium chloride.

Dependence on pH. The effect of pH on k_2 is presented in Figure 6C. Over the entire range, the general trend is an increase in rate of folding as pH is decreased. There are two phenomena which should provide such a monotonic variation over this pH range. The first is the general electrostatic effect of Linderstrom–Lang. As the pH is lowered, the charge on the protein builds up, and it becomes more difficult for the protein chain to assume a compact form. This would tend to decrease k_2 as the pH is lowered. This effect could be very weak in a high ionic strength solution like 3 M guanidinium chloride.

The other effect arises from the interaction with guanidinium ions. As was shown previously, the formation of the transition state from the unfolded state leads to an extensive decrease in the interaction of the protein with guanidinium ions. Since these ions are positive, their elimination becomes easier as the pH is lowered and the positive charge on the protein is increased. This would lead to an increase in k_2 as the pH is lowered. Since it is the latter trend that is observed, the interaction with guanidine appears to dominate over the general electrostatic charge effect.

Figure 6A,B shows the effect of pH on the equilibrium constant and k_1. The minimum in ln K (maximum in stability) at about pH 5.5 is a general property of T4 lysozyme and its mutants (Becktel & Baase, 1987). It has to arise from specific ionic interactions because the isoelectric point of the protein is very high, approximately pH 11. As can be seen from Figure 6B, the same general dependence is found for ln k_1 as a function of pH. Since the minimum appears when the native state is transformed into either the transition state or the unfolded state, and since it does not appear in the transformation from the unfolded state to the transition state, the inference is that the special structural features (buried residues, salt bridges) which produce the minimum are wholly or partially destroyed in the transition state. D. E. Anderson and F. W. Dahlquist (personal communication) have detected and identified at least two strongly abnormal pK's in this protein and are close to a resolution of the problem of its stability as a function of pH. This topic can be discussed more deeply when their analysis is complete.

Conclusions

We will now summarize some of the conclusions we have reached about the nature of the transition state for the unfolding and refolding reaction of this T4 lysozyme, I3C-C97/C54T. It is relatively close to the native state with regard to changes in heat capacity and exposure of groups to solvent (25% and 20% of the way toward the unfolded state for these two criteria, respectively). This indicates that the transition state maintains an extensive system of intramolecular interactions (not necessarily the same as those in the native protein) and is compact. The inference of compactness comes from the fact that extended structures would lead to greater exposure to solvent than was observed. The transition state has a high energy relative to both the native and unfolded states. The energy barrier for refolding comes largely from the formation of hydrophobic interactions which have large positive enthalpies at the low temperatures of these studies. For the refolding reaction, there is extensive enthalpy–entropy compensation, which is also consistent (together with the negative change in heat capacity) with the formation of hydrophobic bonds. For the unfolding reaction, the enthalpy change in going to the transition state is positive which is opposite of expectation for the breaking of hydrophobic interactions. Since no covalent bonds are broken in this process, the conclusion is that there is an extensive breakup of the nonbonded interactions which are responsible for the maintenance of the three-dimensional structure of the protein. The pH studies indicate that the interactions which produce the maximum

stability of the protein at pH 5 are destroyed or greatly reduced in the transition state.

Because all of our studies on this protein resulted in simple kinetics with a single relaxation time, with no perceptible side reactions or slow-folding steps, we have been able to perform an unusually extensive analysis with transition-state theory. This provides a different viewpoint from other studies where the emphasis has been on detecting additional elementary steps in the unfolding or refolding process, or in attempting to discover partially stable intermediates on the folding pathway. One result of this difference in approach is that our results are best expressed in a "state language", i.e., a partial thermodynamic description of the transition state, but with little information on the processes by which the protein goes from its two stable states to the transition state.

It is of interest to compare the properties we have found for the transition state with models which have been proposed for protein folding, though it must be remembered that a number of the suggested models deal with initial steps on the folding pathway and not with the transition state itself, which is the least stable state encountered on the folding or unfolding pathway. In the interpretation of the results, there is a caveat that the kinetics which have been observed are strongly dependent on the concentration of guanidinium chloride. We assume that the effect of this reagent is to lower the free energy of the transition state relative to the native state and not to introduce a new pathway. If this is not the case, we will then have to deal with two mechanisms for folding and unfolding, one in the presence of guanidine and the other in its absence.

There is no direct structural information on the transition state, and with $K^{\ddagger}$ of the order of 10^{-15}, none is likely to be forthcoming. Instead, there are a few thermodynamic parameters and the inferences that can be drawn from them by comparing them with the well-characterized transformation from the native to the unfolded state.

The changes in entropy, heat capacity, and solvent exposure in going from the native to the transition state provide similar information, indicating that the transition state is closer to the native state than the denatured state with respect to these properties, and indicating a partial breakdown of hydrophobic interactions (sign of ΔS, ΔC_p, interaction with guanidine). On the other hand, ΔH is positive and does not conform with the simple breaking of hydrophobic bonds, indicating the disruption of energetically stable nonbonded interactions. These could be associated with both secondary and tertiary structure. The native state is presumably optimized with respect to both nonbonded interactions and hydrophobic bonding.

Unfortunately, measurements which are thermodynamic in nature leave a great deal of latitude in the possible structural interpretation of the results. Any of the following three types of transition state could fit the data that we have obtained. (1) All of the secondary structure is removed. What remains are extensive hydrophobic bonding and nonbonding interactions of a disordered variety. This is not a very attractive candidate for a protein folding model, but it is not excluded by our data. (2) Extensive elements of secondary structure are present in the transition state. These may or may not be identical with those which exist in the native protein. The native tertiary interactions are mostly gone except for extensive, nonspecific hydrophobic interactions. (3) Both secondary and tertiary elements are partially broken down, partially retained, perhaps by an unravelling of the native molecule in one or more places.

Models for protein folding have been recently reviewed by Kim and Baldwin (1982), Harrison and Durban (1985), Ptitsyn (1987), and Jaenicke (1988). We will not describe the models in detail but refer the reader to these sources. The second interpretation above is in accord with the framework model, in which elements of secondary structure are assumed to form prior to reorganization into the native tertiary structure. It is not consistent with a version of this model in which the transition state is considered to consist of elements of secondary structure, unsupported by other interactions, which then coalesce and rearrange to give the native structure. The transition state is compact and possesses extensive hydrophobic interactions.

The results also agree with a sequential folding model, provided the sequence leads to compact rather than extended structures, where the transition state is a relatively late step in the sequence of folding reactions. This would correspond to case 3. Studies of the kinetics of a variety of mutants of T4 lysozyme are under way which should help us test the viability of this model.

Finally, the properties which have been deduced for the transition state, using interpretation 2 above, have much in common with the molten globule state though the latter is not a transition state, but has been observed as a partially stable state of several proteins (Ptitsyn, 1987). Though interpretation 2 and the molten globule state have in common the presence of secondary structure and extensive hydrophobic interactions, they differ in that the latter is a low free energy state which can be transformed to the unfolded state by a noncooperative transformation, while the transition state is a high free energy state associated with the cooperative folding and unfolding reaction.

We conclude that though this study narrows the possibilities somewhat, there remains a broad range of interpretations which we hope to reduce by means of studies of mutants.

ACKNOWLEDGMENTS

We are very grateful to R. Wetzel and L. J. Perry of Genentech, Inc., for the gift of the protein which made this investigation possible. We also thank P. H. von Hippel for the loan of the thermoelectric temperature controller which permitted us to easily extend our measurements to temperatures below 0 °C. We were also aided by discussions with W. J. Becktel, C. G. Schellman, R. L. Baldwin, R. M. Noyes, and F. W. Dahlquist during the course of the investigation.

Registry No. Gdn·HCl, 50-01-1; lysozyme, 9001-63-2.

REFERENCES

Baldwin, R. L. (1986) *Proc. Natl. Acad. Sci. U.S.A. 83*, 8069–8072.

Becktel, W. J., & Baase, W. A. (1987) *Biopolymers 26*, 619–623.

Bevington, P. R. (1969) in *Data Reduction and Error Analysis for the Physical Sciences*, McGraw-Hill, New York.

Brandts, J. F. (1964) *J. Am. Chem. Soc. 86*, 4302–4314.

Brandts, J. F., Halvorson, H. R., & Brennan, M. (1975) *Biochemistry 14*, 4953–4963.

Careri, G., Gratton, E., Yang, P.-H., & Rupley, J. A. (1980) *Nature (London) 284*, 572–573.

Chen, B. (1988) Ph.D. Thesis, University of Oregon.

Chen, B., & Schellman, J. A. (1989) *Biochemistry* (preceding paper in this issue).

Chen, B., Baase, W. A., Nicholson, H., Schellman, C. G., & Schellman, J. A. (1988) *Biophys. J. 53*, 68a.

Crisanti, M. M., & Matthews, C. R. (1981) *Biochemistry 20*, 2700–2706.

Desmadril, M., & Yon, J. M. (1984) *Biochemistry 23*, 11–19.

Garel, J.-R., & Baldwin, R. L. (1973) *Proc. Natl. Acad. Sci. U.S.A. 70*, 3347-3351.
Goldenberg, D. P., & Creighton, T. E. (1985) *Biopolymers 24*, 167-182.
Grathwohl, C., & Wuthrich, K. (1981) *Biopolymers 20*, 2623-2633.
Harrison, S. C., & Durbin, R. (1985) *Proc. Natl. Acad. Sci. U.S.A. 82*, 4028-4030.
Hawkes, R., Grutter, M. G., & Schellman, J. A. (1984) *J. Mol. Biol. 175*, 195-212.
Hermans, J., & Scheraga, H. (1961) *J. Am. Chem. Soc. 83*, 3283-3292.
Ikai, A., & Tanford, C. (1973) *J. Mol. Biol. 73*, 145-163.
Ikai, A., Fish, W. W., & Tanford, C. (1973) *J. Mol. Biol. 73*, 165-184.
Jaenicke, R. (1988) *Prog. Biophys. Mol. Biol. 49*, 117-237.
Kim, P. S., & Baldwin, R. L. (1982) *Annu. Rev. Biochem. 51*, 459-489.
Laidler, K. J. (1950) in *Chemical Kinetics*, Chapter 3, McGraw-Hill, New York.
Matthews, C. R., & Hurle, M. R. (1987) *BioEssays 6*, 254-257.
Northrup, S. H., Pear, M. R., Lee, C.-Y., McCammon, J. A., & Karplus, M. (1982) *Proc. Natl. Acad. Sci. U.S.A. 79*, 4035-4039.
Pace, N. C., & Tanford, C. (1968) *Biochemistry 7*, 198-207.
Pohl, F. M. (1968) *Eur. J. Biochem. 7*, 146-152.
Privalov, P. L. (1979) *Adv. Protein Chem. 33*, 167-241.
Ptitsyn, O. B. (1987) *J. Protein Chem. 6*, 273-293.
Schellman, J. A. (1978) *Biopolymers 17*, 1305-1322.
Segawa, S.-I., & Sugihara, M. (1984) *Biopolymers 23*, 2473-2488.
Sturtevant, J. M. (1977) *Proc. Natl. Acad. Sci. U.S.A. 74*, 2236-2240.
Takagi, T., & Tanford, C. (1968) *Fed. Proc., Fed. Am. Soc. Exp. Biol. 27*, 338.
Tanford, C. (1961) in *Physical Chemistry of Macromolecules*, Chapter 8, Wiley, New York.
Tanford, C. (1968) *Adv. Protein Chem. 23*, 121-282.
Utiyama, H., & Baldwin, R. L. (1986) *Methods Enzymol. 131*, 51-70.
Weaver, L. H., & Matthews, B. W. (1987) *J. Mol. Biol. 193*, 189-199.
Wyman, J. (1964) *Adv. Protein Chem. 19*, 223-286.

NMR Studies of the Influence of Dodecyl Sulfate on the Amide Hydrogen Exchange Kinetics of a Micelle-Solubilized Hydrophobic Tripeptide†

Joe D. J. O'Neil and Brian D. Sykes*
MRC Group in Protein Structure and Function, Department of Biochemistry, University of Alberta, Edmonton, Alberta T6G 2H7, Canada
Received August 1, 1988

ABSTRACT: Backbone amide hydrogen exchange measurements are an important source of information about the internal dynamics of proteins. Before such measurements can be interpreted unambiguously, contributions to hydrogen exchange rates from the chemical and physical environment of the amides must be taken into account. Membrane proteins are often solubilized in detergents, yet there have not been any systematic investigations of the possible effects detergents may have on the amide hydrogen exchange rates of proteins. To address this question, we have measured individual backbone and carboxyl-terminal amide exchange rates for the amphipathic tripeptide Leu-Val-Ile-amide dissolved in water and dodecyl sulfate micelles. ^{1}H NMR spectroscopy was used to measure exchange using the direct exchange-out into D_2O technique at 5 °C and using an indirect steady-state saturation-transfer technique at 25 °C. The broadening effect of micelle-incorporated spin-labeled fatty acid (12-doxylstearate) on the ^{1}H NMR spectra of both the detergent and the peptide resonances was used to demonstrate that the tripeptide is intimately associated with the micelle. The resonance from formate ion, which is excluded from the micelle, was unperturbed by the spin label. The detergent did not retard the exchange rates of either the primary (terminal) or secondary (backbone) amides of the tripeptide. This suggests that the micelle/peptide interaction does not restrict access of charged catalysts and water to these amides and shows that the peptide amides are not hydrogen bonded. However, the pH for the exchange minima of these amides in detergent was increased between 1.2 and 1.7 units compared to exchange in water. This is due to the electrostatic effect of the negative charge on the sulfate groups that concentrate protons in their vicinity, effectively lowering the pH in the microenvironment of the amides. These experiments help to explain the elevated pH_{min} observed for backbone amides in the sodium dodecyl sulfate solubilized M13 coat protein [O'Neil, J. D. J., & Sykes, B. D. (1988) *Biochemistry 27*, 2753-2762].

Characterizing the dynamic aspects of protein structure will undoubtedly contribute to a better understanding of the mechanisms that enable proteins to carry out their biological functions. Among the several experimental approaches to the analysis of protein dynamics [for a review see Karplus and McCammon (1981)] is the measurement of polypeptide backbone amide hydrogen exchange rates. Linderstrøm-Lang (1955) and his colleagues (Hvidt & Linderstrøm-Lang, 1954; Linderstrøm-Lang & Schellman, 1959) first recognized that amide exchange rates are in some way determined by protein structural fluctuations. However, hydrogen exchange rates

†Supported by the Medical Research Council of Canada (MRC Group in Protein Structure and Function) and the Alberta Heritage Foundation for Medical Research (J.D.J.O. is the recipient of an AHFMR Postdoctoral Fellowship).

0006-2960/89/0428-0699$01.50/0